

Model Development for Numerical Simulation of Aortic Blood Flow

Wael Mokhtar, Clayton Spore, Bhagawan Upreti, and Spencer Boer

School of Engineering, Grand valley State University,
Grand Rapids, Michigan, USA.

I. Abstract

The ascending aorta is the main artery which supplies all the systemic circulation in the human body. Computational Fluid Dynamics (CFD) can be used to investigate a number of different phenomena that occur during the cardiac cycle, such as blood flow and shear stress on the walls of the aorta. In order to accurately assess these cardiac behaviors, standard computational techniques were used. CFD typically consists of three major steps; pre-processing, solving, and post-processing. Pre-processing, or model development, has a significant effect on the accuracy and scope of the results of a CFD study. Consequently, the focus of this paper is on the model development for aortic blood flow in healthy cardiac patients. The particular emphasis of this paper is comparing three different aorta models. Three different geometric reconstructions were developed, representing aortic passageways obtained from CT scan data. The models used were an optimized CT aorta model, an unrefined CT aorta model, and an idealized tube model. From the model development it was determined that a smoothed representation of CT scan data most accurately represents the blood flow velocity and distribution, as well as aortic wall shear stresses. This model represents a basis for further refinement and application in clinical aortic blood flow research.

II. Introduction

The aorta is the largest artery in the human body, beginning at the left ventricle of the heart. It is a tube like structure having approximate length of a foot and diameter of an inch. Blood is pumped by the heart into the aorta through the aortic valve. The three leaflets in an aortic valve opens and closes with each heart beats and prevents the backflow of the blood [1]. The aorta is divided into three major sections; ascending aorta, aortic arch, and descending aorta. The aorta begins as the ascending aorta, which turns into the aortic arch. The aortic arch then leads to the descending aorta. The aortic arch has a steep curvature and typically joins the ascending and descending aorta. The descending aorta can be further divided into thoracic aorta and abdominal aorta. It begins as a thoracic aorta, runs from heart to the diaphragm and enters the abdominal region becoming an abdominal aorta. which runs until the aortic bifurcation [2]. Figure 1 depicts region identification for the aortic region.

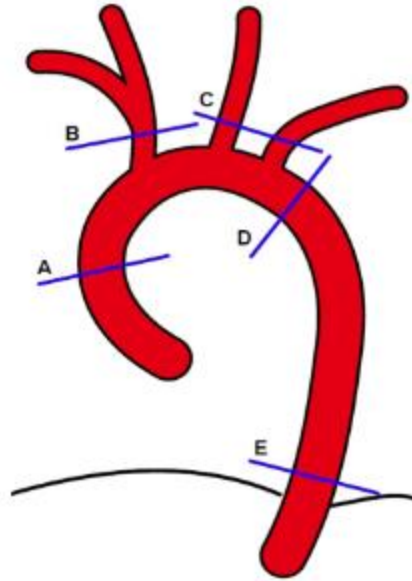


Figure 1: Aorta Nomenclature: Ascending Aorta (A), Brachiocephalic Artery (B), Left Carotid Artery (C), Left Subclavian Artery (D), Descending Aorta (E)

The phenomenon of blood flow in aorta is very complex. Blood flow pattern may depend on the viscous properties of the blood, elasticity of the aorta, the propagation and reflection of the shock waves generated during ventricular contraction, the entrance region effects in aorta [3]. However, one commonly accepted fact is that the blood flow pattern in aorta begins with high blood pressure, increasing the pressure wave of the blood against the wall; and the pressure gradually drops down as the blood progresses forward. Blood flow is turbulent only in the ascending aorta region during the states of higher cardiac output [4]. The blood flow also depends on the aorta model developed for study. The CT scan of the aorta can be used to develop the anatomical model. Small jagged surfaces and fillets, and the roughness present in the unrefined model affects the flow characteristics to large extent. The flow in the refined model is expected to be smoother than the rough model developed by using some commercially available software.

III. Literature Review

LaDisa et al. performed CFD evaluation of aortic coarctation using data obtained directly from MRI patient data. In the model developed, a three-element Windkessel model was imposed to represent the impact of distal vessels [1]. Mokhtar evaluated the effect of cannulation angle on the creation of emboli using computational fluid dynamics. In this study, criteria evaluated were wall shear stress, normal stress, intra-fluid shear stress and flow distribution in the region of cannulation [2]. Svensson et al. completed a feasibility study using CFD simulation to assess the aortic blood flow distribution using magnetic resonance imaging. In this feasibility study, inlet boundary conditions was extracted directly from MRI data [3]. Simão et al. used CFD simulation tools to predict possible anomalies in ascending aorta aneurysms from patient data. Models were extracted using CT scan data in combination with COMSOL software and ignored the effects of wall motion on velocity and arterial wall shear stress [4]. Ku discussed the techniques, challenges and effects of blood flow in arteries. In this paper, the effects of various stresses on arterial walls was discussed in addition to the biological responses to hemodynamics [5].

Picone et al. Estimated aortic SBP from brachial MAP/DBP calibration of radial waveforms had a significantly smaller mean difference than from brachial SBP/DBP calibration (-0.7 ± 7.5 mmHg versus -6.9 ± 7.3 mmHg, $P < 0.0001$ for difference). Of the other calibration methods, estimated aortic SBP was most accurate from aortic MAP/DBP calibration of radial waveforms (-1.8 ± 5.0 mmHg, $P = 0.00023$). [8] Shin et al. created a 3D aortic model using CT images that imported into the 3D segmentation using Mimics software and applied a pulsatile blood pressure waveform for the ascending aorta to provide a biomimetic environment [9] Morris et al. used the flow rates were obtained from Nichols and O'Rourke for the ascending aorta and the input velocity based on this flow rate is shown in. The time average input velocity was 0.059m/s with a maximum input velocity of 0.262m/s occurring at 0.137 sec. The maximum acceleration and deceleration occurred at 0.078 sec and 0.379 sec respectively. [10,11].

Simão, M et al.(2017) showed that the low wall shear stress results in the blood stagnation in the ascending aorta and the low Wall Shear Stress areas coincide with the location of recirculation zones, related to low velocities [7]. Klipstein, R et. al., (1987) showed that the blood flow during systole is one way whereas during diastole, blood flow in ascending aorta shows forward and reverse pattern [12]. Stein, P., & Sabbah, H. (1976) concluded in their study that the turbulent flow in healthy person's aorta occurs only in ascending aorta during high cardiac output [13]. This result is again rephrased by Klipstein, R et. al., (1987) in their study of blood flow pattern in human aorta by magnetic resonance [14]. However, none of them have mentioned and compared the blood flow characteristics in different aorta model fidelities.

IV. Extraction Process of CAD from CT Scan Data

The process which created the aorta models in this paper was done using the software Materialise Interactive Medical Image Control System (Mimics). In order to generate a useable anatomical 3D model for CFD purposes this software was chosen due to its medical capabilities and tools. The software uses CT scan data and other user input to segment anatomical regions and in turn create a geometric 3D model. Mimics is able to automatically generate 3D models but strategies and methodology is required to extract a much cleaner model. The semi-automatic method required creating a bounding box to better isolate the aorta and creating a mask which will be applied over a specific range of Hounsfield Units (HU). Hounsfield Units make up the grayscale on CT images and can be assigned 4096 different values. Given a pixel from black to white the software will assign it a value and then the user is able to apply a mask and automatically filter regions in a desired HU range. This enables Mimics 3D generation tool to separate fat, bone, and muscles from one another. Once the mask is applied, additional refinement of the mask is often necessary to separate bone from bone or muscle from muscle, regions that connect to each other with similar HU values. In this case additional mask modification was necessary to separate the aorta further. Mimics was able to do this by splitting the mask by using a number of user selected and spaced out CT scans in which the user highlighted the bounds of the aorta. Using this methodology a useable aorta model was able to be extracted with minimal and small scale additional clean up required. With no changes made from this methodology the unrefined CT aorta model was created. The refined CT aorta model was created using smoothing and clean up on this unrefined model.

Some of the potential errors and assumptions made in the model generation comes from the nature of image segmentation. A CT scan is a segmenting scan as an image slice is taken then the machine will increment a few millimeters before another image is taken. This means very small

geometries can be missed in the recreation of the anatomical 3D model. However, this segmentation is what makes the series of images easier to analyze and digest. The small geometries that are theoretically missed are accounted for in the geometric generation by using interpolation algorithms in between the series of slices.

V. Presentation of Model Fidelities

For accurate CFD flow prediction of human blood flow distribution, model fidelity and surface quality plays a pivotal role. For application to patient cases, the model must accurately represent the surface roughness and undulation. In this study, three levels of model fidelities were utilized to determine the model most representative of human arteries. The three models used for study were an unrefined aorta model, smoothed aorta model and idealized aorta model. The unrefined aortic model was directly extracted from the CT data without any additional surface refinements or smoothing. Figure 2 below depicts the unrefined aorta model.



Figure 2: Unrefined CT Aorta CAD Model

The unrefined aorta model has high irregularity and roughness of the aortic surface. This geometry has a significant potential for disturbing blood flow and disrupting the blood flow pattern. As the model was extracted without secondary smoothing processes, this model has localized peaks and valleys, typically not observed on human aortic walls. The irregular surface condition will have negative effects on the formation of the CFD mesh utilized for analysis, particularly in regions closest to the wall boundary. Due to the lack of refinement and smoothing, the unrefined model is the closest representation of the extracted CT scan data for the patient. Investigation into the negative effects of irregular surface condition will be pivotal for determination of the most accurate model. To reduce the surface roughness, smoothing algorithms were applied in the Mimics software package to create the smoothed CT aorta model (Figure 3)



Figure 3: Smoothed CT Aorta CAD Model

The smoothed aorta model has significantly reduced wall roughness and irregularity. It should be noted that the smoothed aorta model is a refined derivative of the unrefined aorta model. Upon conversation with medical professionals, the surface regularity and smoothness for this model appears to be most indicative of human aortic walls [6]. Due to this, the smoothed model is expected to replicate human blood flow distribution most accurately. Mesh generation and boundary layer development for the smoothed model will be more uniform than its unrefined counterpart. As the wall condition will have a significant effect on shear stress, pressure gradients and blood flow, a further refinement of the wall boundary was developed for investigation. Figure 4 depicts the idealized model for the CT scan of a patient's aorta.

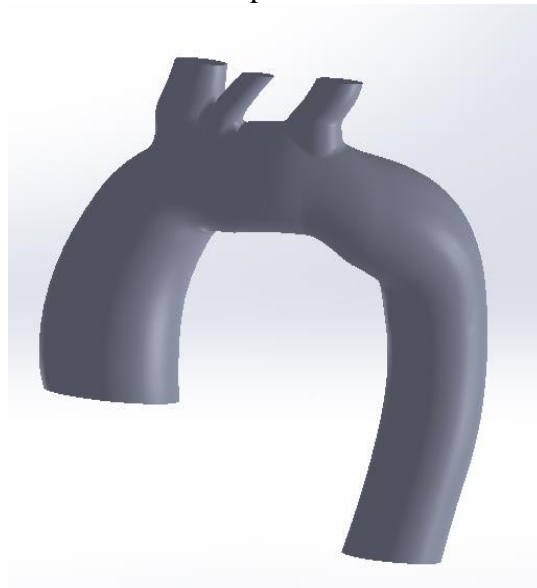


Figure 4: Idealized CT Aorta CAD Model

This model was generated using Solidworks surface modeling techniques and represents an idealized surface boundary condition. This idealized model will reduce irregularity and randomness in the fluid flow generated by the surface condition. The absence of jagged surfaces may lead to a reduction of wall shear stress and fluid back pressure. This idealized model may be an oversimplification of the human aorta. This investigation will determine which model is representative of human aortas and will be used in further investigative CFD modeling work.

VI. CFD Model Development

a. Mesh Conditions

Models selected for mesh generation of the ascending aortas were surface remesher, trimmer, and prism layer mesher. Prism layer mesher to accurately capture the boundary layer of the fluid. Representation of the fluid boundary layer is crucial for accurate blood flow at the aortic wall. As mentioned previously, CAD was generated using CT scan data, Materialise Mimics and SolidWorks 2018. This combination of software ensured that geometry inputs to StarCCM were error free. This allowed the use of surface remesher model, as discontinuities or singularities in the geometry were not present. Localized refinements were applied to the pressure outlet boundaries to reduce the effect of boundary condition error. Figures Figure 5Figure 6 show the mesh representation used for model analysis.



Figure 5: Volume Mesh: Smoothed (Left), Untouched (Middle), Idealized (Right)

As shown, a mesh with adequate density to capture aortic wall interaction was developed for the three models to be analyzed. The parameters input to the mesh models for the three levels of CAD fidelity were identical. Clustering near boundaries was included to ensure accurate results. The final volume mesh for the smoothed model contained 3,888,165 cells with 11,263,858 interior faces. The final volume mesh for the untouched model contained 5,088,281 cells with 14,828,198 interior faces. The final volume mesh for the idealized model contained 3,784,513 cells with 10,938,496 interior faces. The untouched mesh generated a significantly larger number of cells and interior faces. This is due to the irregularity of the imported surface, resulting in more clustered cells near the boundary. Figure 6 shows that there is minute variation in the profile in the aortic arch for all three models.

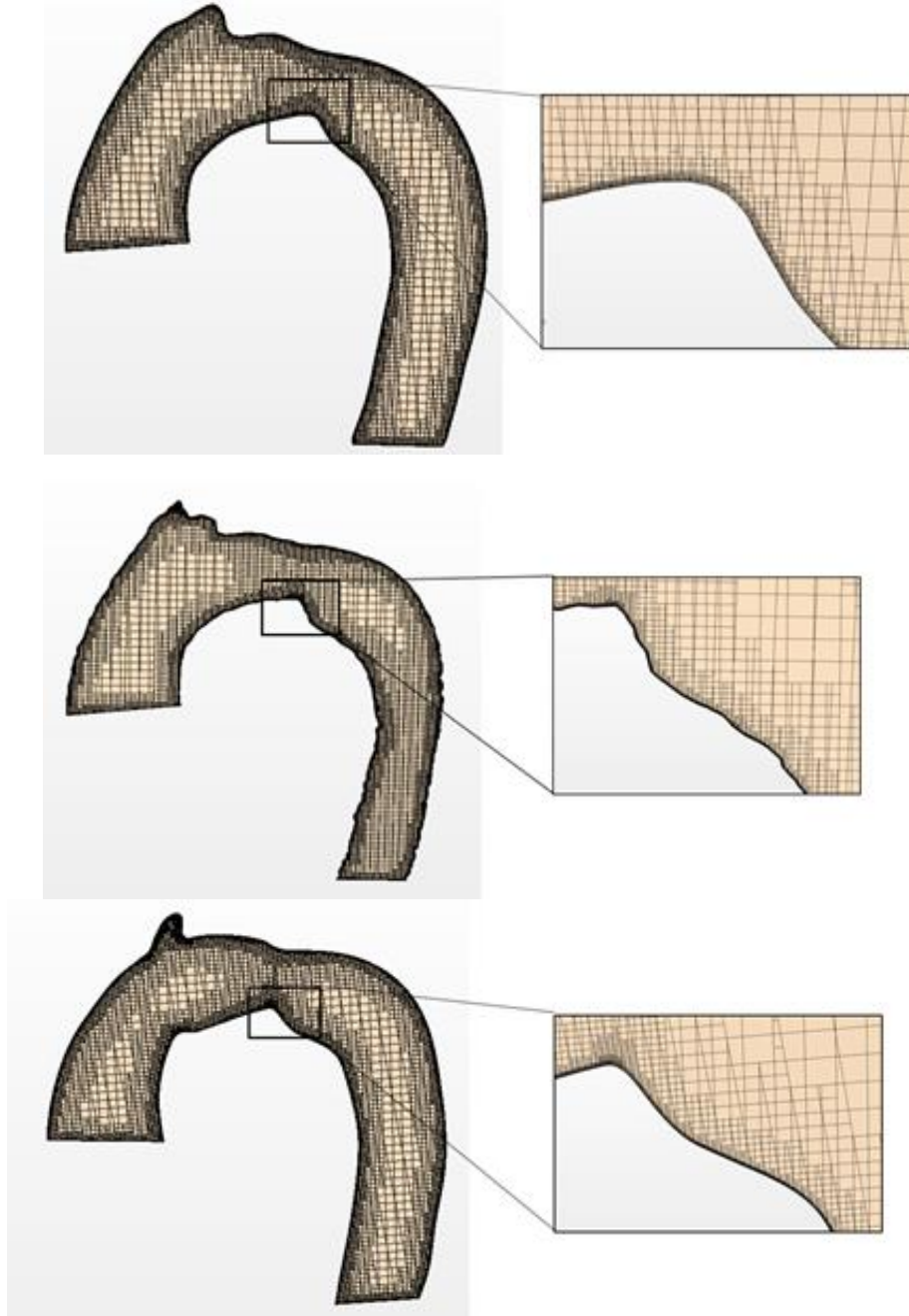


Figure 6: Volume Mesh: Smoothed (Top), Untouched (Middle), Idealized (Bottom)

b. Physics Conditions

This CFD evaluation used a three dimensional steady state model to analyze velocity profiles, mass flow distribution and wall shear stress variation between three levels of patient scan data representation. In this fluid dynamics study, blood was treated as a water with adjusted, constant, density. The model presented treats the blood as a Newtonian fluid. Further studies could be performed to evaluate blood as a true non-Newtonian fluid. The density used for the blood was

1101.45 kg/m³ [2]. Due to the irregularities of the mesh for the untouched model, a coupled solver was used for better convergence. The turbulence of the fluid was modeled with realizable k-ε two-layer turbulence model. This model was chosen as the two-layer treatment near the wall boundary and far from the wall boundary accurately capture the interaction of the blood flow and the aortic walls, while retaining mass blood flow through the aorta. Figure 7 below shows the boundary conditions applied for this evaluation.

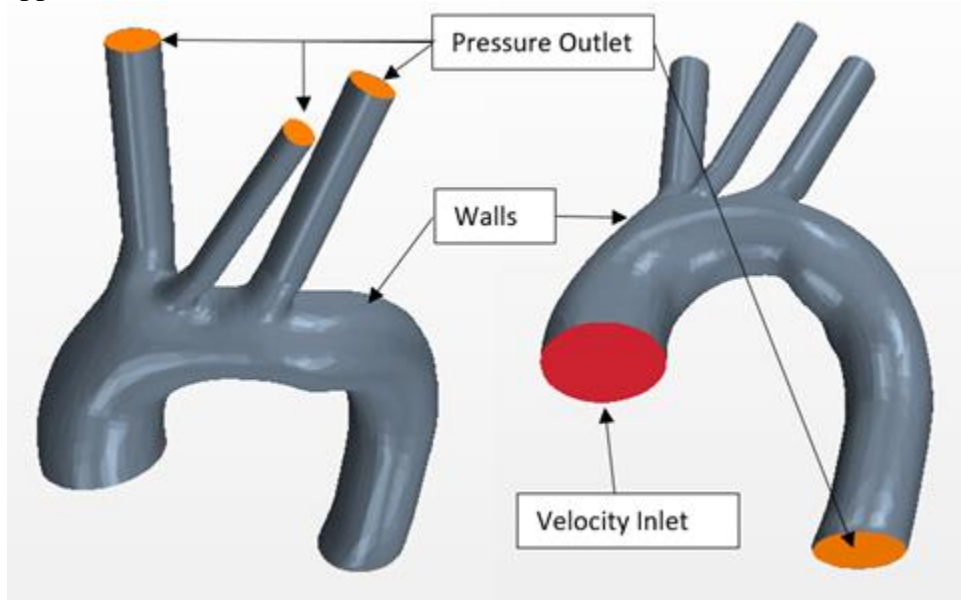


Figure 7: Model Boundary Conditions

The boundary conditions presented in Figure 7 were applied to all three models. Due to the pulsatile nature of aortic blood flow, velocity, pressure and wall shear stress are a transient behavior. Peak velocities, pressures and shear stresses are expected to occur during the systole of the heartbeat. Consequently, the inlet velocity used for this steady state analysis was peak systole velocity for a healthy human heart, 0.1 m/s [1, 6]. As blood flow is primarily unidirectional, the lower region of the ascending aorta, or sinotubular junction, was treated as the velocity inlet. The descending aorta, brachiocephalic trunk, and left common carotid artery were treated as pressure outlets. Remaining surfaces of the aorta were treated as wall boundaries. Table 1 below shows blood flow distribution for healthy males and females ranging in age from seventeen to forty [7].

Table 1: MRI Blood Flow Data [7]

Location	% Blood Flow		
	Average	Min	Max
Ascending Aorta	100%	100%	100%
Descending	59.1%	47.8%	87.3%
Brachiocephalic	18.7%	12.3%	29.2%
Left Carotid	6.8%	3.8%	9.9%
Left Subclavian	10.0%	5.3%	15.8%

Results/ Discussion

Simulations were completed using STARCCM+ v13.04.011. CFD results of interest aortic simulations include blood flow distribution and stresses applied to arterial walls. Blood flow distribution within the aorta has significant impact on blood circulation within the body. Consequently, developed models must accurately predict blood flow to various aortas and arteries. Additionally, shear stresses can have significant negative effects on the vascular tissue. For this reason, the model developed must accurately represent shear stress distribution along arterial or aortic walls. Figure 8 shows the streamline velocity of the blood within the aorta.

As shown below, all three models show similar blood flow patterns, but the quality of the exterior surface has a notable effect on the velocity profile. Average blood flow velocity is highest for the idealized model, which has perfectly regular wall boundary conditions. The untouched model displayed the lowest average velocity, while the smoothed model fell in between. This trend is a direct result of the loss of fluid momentum due to surface irregularity. The untouched model, which contains a significant number of rough or jagged surfaces, which directly impedes and disrupts blood flow. In contrast, the idealized model exhibits minimal boundary condition disruptions, leading to a higher average velocity profile. As human aortas form irregularities due to other organs, damaged tissues or other factors the idealized model may not capture the wall boundary condition accurately. Additionally, the untouched model represents the opposite side of the spectrum, with wall boundary conditions unrealistic of a healthy human aorta or artery. All three models predict a region of blood flow acceleration in the aortic arch. This acceleration is due to a constriction of the aorta. This acceleration, and consequential low pressure region, forces blood flow into the brachiocephalic trunk, left subclavian and left carotid arteries. All three models predict a large region of blood flow separation and recirculation in aortic arch. Figure 9 shows the various plots of blood flow recirculation in these regions.

These recirculation regions, are directly related to the blood velocity and aortic profile. As shown above, the faster the blood flow is traversing through the aorta, the larger the region of recirculation will be. This region of recirculation is only present along the centerline due to the sharp nature of the geometric transition in the aortic arch. These regions of recirculation can have negative consequences on blood flow to the lower region of the body. Table 2 shows the distribution of blood flow to the descending aorta and brachiocephalic trunk, left carotid, left subclavian arteries.

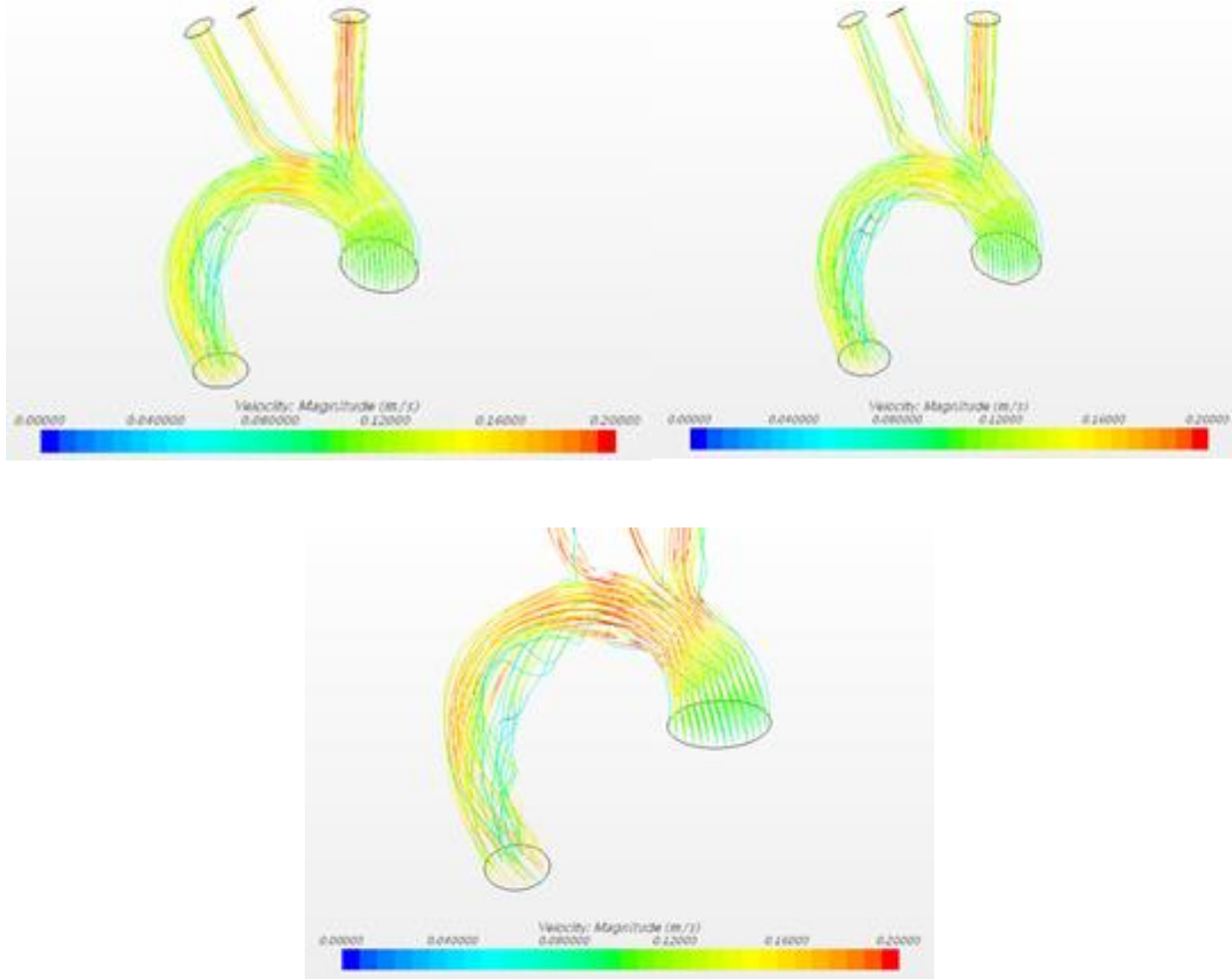


Figure 8: Velocity Streamlines: Smoothed (Top), Untouched (Middle), Idealized (Bottom)

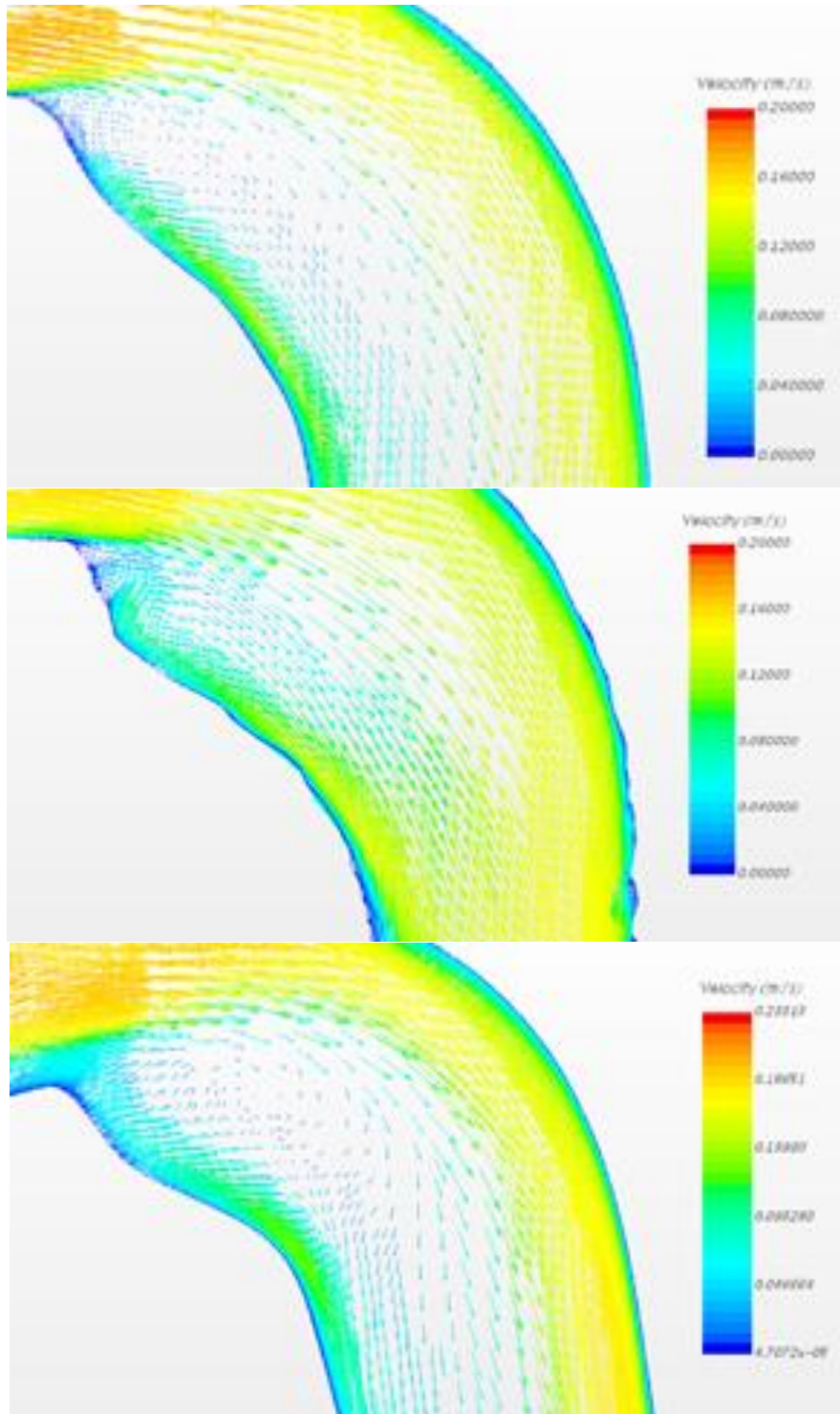


Figure 9: Vector Velocity Blood Recirculation Zone: Smoothed (Middle), Untouched (Middle), Idealized (Bottom)

Table 2: Aortic/ Arterial Pressure Outlet Mass Flow Distribution

Location	Smoothed		Untouched		Idealized	
	Blood Flow (kg/s)	% Blood Flow	Blood Flow (kg/s)	% Blood Flow	Blood Flow (kg/s)	% Blood Flow
Ascending Aorta	0.1302	100.0%	0.128	100.0%	0.1346	100.0%
Descending	0.0718	55.1%	0.0648	50.6%	0.0699	51.9%
Brachiocephalic	0.0286	22.0%	0.0285	22.3%	0.0296	22.0%
Left Carotid	0.009	6.9%	0.0103	8.0%	0.009	6.7%
Left Subclavian	0.0209	16.1%	0.019	14.8%	0.0221	16.4%

Blood flow distribution to descending aorta and brachiocephalic trunk, left carotid, left subclavian arteries is pivotal for circulation and health. Compared to the data presented in Table 1, the models developed capture the trend of blood flow distribution well. From the models developed, only two blood flow predictions fall outside of Muellers data. The two blood flow predictions that fall outside of the established range for healthy adults were the smoothed and idealized left subclavian blood flows. The smoothed model predicted 16.1% left subclavian blood flow while the idealized model predicted 16.4% blood flow. This is compared to a range of 5.3-15.8% published by Mueller [7]. This error may be attributed to arterial backpressure not being modeled at the pressure outlet boundary conditions. To improve the accuracy of the simulation for future use, these values should be determined and implemented. Figure 10 depicts the predicted shear stress distribution along the aortic and arterial walls.

Analyzing the shear stress distribution for the three models developed it is clear that wall irregularity of the untouched model overpredicts shear stress. This is due to the jagged and rough boundary that interacts with the blood. The idealized and smoothed models more realistically predict the shear stress distribution on the aortic wall. The smoothed model does not exhibit localized spikes in shear stress, indicative of actual aortic wall behavior. Consequently, the smoothed model most realistically predicts blood flow interaction with the aortic wall.

Utilizing the results of this model development study, accurate representation of a human aortic section from CT scan extraction is possible. The results of this study can be implemented for non-invasive investigative work in the medical field. Using the developed model and patient CT scan data, trained medical professionals will be able to optimize planned procedures. An example of this models future utility is the implementation of blood flow prediction for assistive heart pumps, or Ventricular Assist Device (VAD). This will allow surgeons to investigate the effects of VAD devices and VAD inlet locations on blood flow distribution, while reducing negative health risks associated.

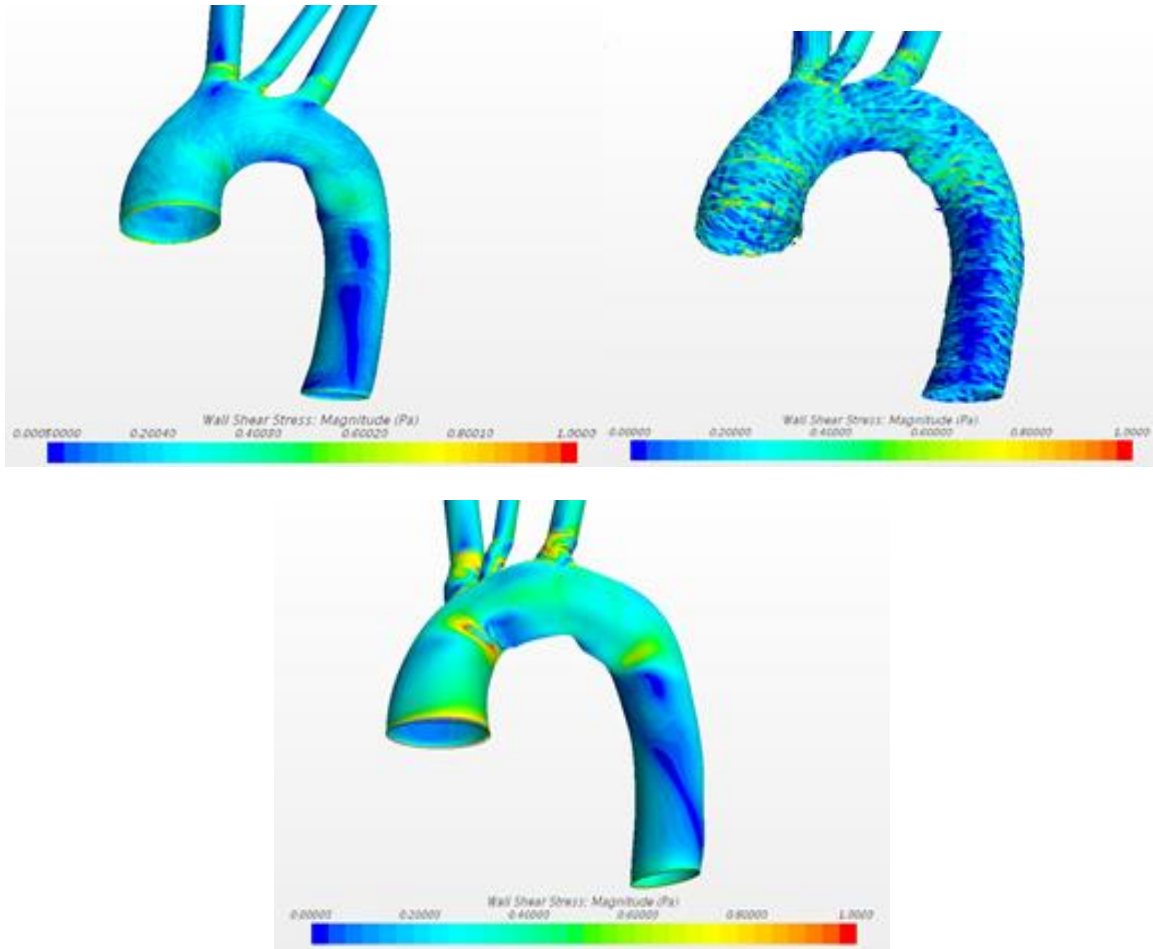


Figure 10: Scalar Velocity Profile Along Aortic Centerline: Smoothed (Left), Untouched (Right), Idealized (Bottom)

VII. Conclusions

The conclusions of this study are focused around the blood flow, its distribution, and the shear stress seen in the differing aorta models. From the results of the simulations it was seen that the wall surface irregularities impacted the blood flow by reducing fluid momentum. The idealized model was perfectly smooth and had no jagged edges like the untouched model that has edges that disrupt fluid flow. As a result of this the idealized model predicted the highest average velocity whereas the untouched model predicted the lowest. Leaving the smoothed model in between the two velocities as intuitively expected. Some of the geometric impact on the fluid flow comes from the restriction region at the aortic arch. Due to the constriction of the aorta the blood flow velocity is increased in this area which results in blood being forced into the brachiocephalic trunk, left carotid, and left subclavian arteries. This is due to the low pressure regions in this area. The area just following the aortic arch contained large recirculation regions in all three models. The largest of these regions was in the idealized model where velocity was the largest and smallest in the untouched model. This area of recirculation is present along the centerline and can have a negative effect on blood flow to the lower half of the body. However, compared to data obtained by Mueller

[7] it was determined that each of the models captured the distribution of blood flow well. The numbers that were calculated for the blood flow in each region of interest mostly fell within the range of a healthy adult, with the exception of two flows. The two blood flows that did not fall within the range presented by Mueller as previously mentioned were the smoothed and idealized left subclavian blood flows. In the smoothed and idealized cases the blood flow seems to be overestimated as the distribution is at 16.1% and 16.4% respectively, compared to the 5.3%-15.8% published range. This could be due to backpressure not being modeled at the pressure outlets in the model and will be addressed in the future studies section. Apart from fluid flow the shear stress on the walls of the aorta is also an area of interest as it impacts the strength of the aorta. Across the three models it was seen that the jagged surfaces like those on the unsmoothed model resulted in a number of localized spikes of wall shear stress. This is an unrealistic prediction from what is known about the geometry and behavior of the “average” aorta. The models that were seen to realistically represent the shear stress were the smoothed and idealized cases. The most realistic of differing surface qualities was the smoothed case as it is refined enough to eliminate localized spikes and not oversimplifying the geometry of an aorta which is non perfectly smooth.

VIII. Future Studies

Future work in this area will be taking the quality criteria now determined for modelling an aorta and improving upon it. As it was discovered in the results of the simulations the blood flow distribution in the left subclavian artery was overestimated in the smoothed and idealized cases. With the smoothed aorta case being the most realistic case, being able to match the simulation with data obtained from literature would eliminate some of the drawbacks of the model. Future studies should include backpressure on the pressure outlets in the model. This will involve determining the values from literature and implementing them into the simulation. Making this change will improve the accuracy of the model and in theory eliminate the error that was found in the blood flow in the left subclavian artery. Other future work could involve evaluating the models using blood as a non-newtonian fluid. In this study blood was treated as water with an increased density, pertaining to the density of blood. But with this fluid being simplified as a newtonian fluid actual behavior of blood in this environment could be overlooked. Once these changes are made a “standard” aorta quality criteria can be used in future studies involving the aorta. This model criteria could serve as a baseline model in order to verify results when changes are made to the aorta.

IX. Acknowledgements

This paper was supported directly by the School of Engineering at Grand Valley State University, whom have provided resources, funding and guidance. The authors gratefully acknowledge Dr. David Langholtz, Medical Director of Richard and Helen DeVos Cardiac Diagnostic Unit, Frederick Meijer Heart and Vascular Institute, for his vital guidance and support towards the team.

References

1. Ladisa, J. F., Figueroa, C. A., Vignon-Clementel, I. E., Kim, H. J., Xiao, N., Ellwein, L. M., Taylor, C. A. (2011). Computational Simulations for Aortic Coarctation:

- Representative Results From a Sampling of Patients. *Journal of Biomechanical Engineering*, 133(9), 091008. doi:10.1115/1.4004996
2. Mokhtar, W. (2017). Effect of Negative Angle Cannulation during Cardiopulmonary Bypass - A Computational Fluid Dynamics Study. *International Journal of Biomedical Engineering and Science*, 4(2), 01-13. doi:10.5121/ijbes.2017.4201
 3. Svensson, J., Gårdhagen, R., Heiberg, E., Ebbers, T., Loyd, D., Länne, T., & Karlsson, M. (2006). Feasibility of Patient Specific Aortic Blood Flow CFD Simulation. *Medical Image Computing and Computer Assisted Intervention – MICCAI 2006 Lecture Notes in Computer Science*, 257-263. doi:10.1007/11866565_32-
 4. Simão, M., Ferreira, J., Tomás, A. C., Fragata, J., & Ramos, H. (2017). Aorta Ascending Aneurysm Analysis Using CFD Models towards Possible Anomalies. *Fluids*, 2(2), 31. doi:10.3390/fluids2020031
 5. Ku, D. N. (1997). Blood Flow In Arteries. *Annual Review of Fluid Mechanics*, 29(1), 399-434. doi:10.1146/annurev.fluid.29.1.399
 6. Langholtz, D. (2018, December 5). Spectrum Doctor Team Interview [Personal interview].
 7. Mueller, T., Rengier, F., Muller-Eschner, M., Kotelis, D., Geisbusch, P., Kauczor, H. U., & Von Tengg-Kobligk, H. (2012). Supra aortic blood flow distribution measured with phase-contrast MR angiography. *European Society of Radiology*.
 8. Picone, D. S., Schultz, M. G., Peng, X., Black, J. A., Dwyer, N., Roberts-Thomson, P., . . . Sharman, J. E. (2019). Intra-arterial analysis of the best calibration methods to estimate aortic blood pressure. *Journal of Hypertension*, 37(2), 307-315. doi:10.1097/hjh.0000000000001902
 9. Shin, E., Kim, J. J., Lee, S., Ko, K. S., Rhee, B. D., Han, J., & Kim, N. (2018). Hemodynamics in diabetic human aorta using computational fluid dynamics. *Plos One*, 13(8). doi:10.1371/journal.pone.0202671
 10. Morris, L., Delassus, P., Callanan, A., Walsh, M., Wallis, F., Grace, P., & Mcgloughlin, T. (2005). 3-D Numerical Simulation of Blood Flow Through Models of the Human Aorta. *Journal of Biomechanical Engineering*, 127(5), 767. doi:10.1115/1.1992521
 11. McDonald, D. A., Nichols, W. W., ORourke, M. F., & McDonald, D. A. (1990). *McDonalds blood flow in arteries*. Edward Arnold.
 12. Hoffman, M. (n.d.). The Aorta (Human Anatomy): Picture, Function, Location, and Conditions. Retrieved from <https://www.webmd.com/heart/picture-of-the-aorta#1>.
 13. Klipstein, R., Firmin, D., Underwood, S., Rees, R., & Longmore, D. (1987). Blood flow patterns in the human aorta studied by magnetic resonance. *Heart*, 58(4), 316-323. doi:10.1136/hrt.58.4.316
 14. Stein, P., & Sabbah, H. (1976). Turbulent blood flow in the ascending aorta of humans with normal and diseased aortic valves. *Circulation Research*, 39(1), 58-65. doi:10.1161/01.res.39.1.58